Monodispersed metal clusters in solid matrices: A new experimental setup

Matthias Hillenkamp,* Giulia di Domenicantonio, and Christian Félix
Insitut de Physique des Nanostructures,
École Polytechnique Fédérale de Lausanne
CH-1015 Lausanne-EPFL, Switzerland
(Dated: January 10, 2006)

We describe a new experimental setup for the production of samples of metal clusters embedded in matrices stable at ambient conditions. The cluster ions are generated in the gas phase and co-deposited fragmentation-free together with the evaporated matrix. Mean cluster sizes range from a few to many thousands of atoms. For small clusters ($n < 20$) mass selection is possible, larger clusters are deposited in narrow size distributions. Matrix materials include metals (Cu, Ag) and oxides such as quartz. The performance of the apparatus as well as sample characterization procedures are described. We show first results on the magnetic properties of different cobalt cluster size distributions ($\langle n \rangle = 15, 600, 2300, 6500$) embedded in copper matrices, demonstrating inter-cluster as well as cluster-lattice interactions.

PACS numbers: 36.40.Cg, 36.40.Vz, 61.46.+w, 75.75.+a, 78.67.-n
Keywords: metal cluster, matrix, magnetism, spectroscopy, cobalt, copper, mass selection

I. INTRODUCTION

The electronic and magnetic properties of metal clusters in the gas phase as well as supported on surfaces have attracted attention since many years and a lot of both experimental and theoretical work has been devoted to this field. However, in almost all possible applications of metal clusters, nanostructured bulk systems providing sufficient thermal, mechanical and chemical stability are needed. There has consequently been considerable research on metal nanoparticles in solid and stable matrices such as glasses, metals, semiconductors and the like. The aim is to be able to specifically tailor the properties of a device by controlling e.g. composition, size and concentration of the embedded clusters.

This is exemplified by several recent publications: The group of Dickson has measured fluorescence and electroluminescence of silver nanoparticles in an oxide matrix [1]. The observed fluorescence is attributed to small metal clusters produced by either ohmic or optical activation. A detailed characterization of both the cluster and its chemical surroundings, however, is not yet available. It is nevertheless possible to perform single particle spectroscopy as well as simple logical operations with these samples [2, 3], demonstrating the relevance and potential for future applications.

At the same time a lot of work is devoted to magnetic nanostructures and their possible applications [4–6]. One of the benchmark systems in this context has always been Cobalt in Copper which is well suited due to the bulk immiscibility of the two components below 400^oC, preventing homogenous alloying [7].

Most of the experimental work on granular systems published so far has been on samples with very broad particle size distributions, e.g. with rapidly cooled melts, melt-spun ribbons or co-sputtered thin films [8, 9]. By annealing the samples further precipitation of Co can be induced. Obviously any size effects that are expected to be very important, especially for small particles in the nm-regime, are blurred out in samples like these. Also it is practically impossible to independently vary two of the most important factors: particle size and concentration. In the last few years several groups have developed experiments in order to at least narrow down size distributions and to independently control the concentration by co-depositing preformed clusters and the atomic matrix. Issues addressed in these experiments were e.g. the cluster magnetic moments [10], their anisotropy [11] and the influence of cluster interfaces on the giant magnetoresistance [12].

While these experiments already allow a much better understanding of the magnetism of nanostructured systems, they remain restricted to cluster sizes with $d > 2nm$ ($\sim 550 atoms$). It is normally the whole neutral cluster size distribution which is deposited without size selection [13]. Up to date, no experimental data on the optical or magnetic properties of well defined smaller clusters in solid matrices (with the exception of rare gases) exist, especially not on size selected systems.

This lack of experiments is aggravated by the fact that a comparison to theory remains extremely difficult. In order to pin down exactly cluster size effects elaborate spin density functional calculations including RKKY interactions are necessary. Several publications are already available, but due to the complexity of the systems in question, only very restricted cluster sizes have been calculated (see e.g. [14–18] for up to 55 atoms per cluster).

*Electronic address: matthias.hillenkamp@epfl.ch

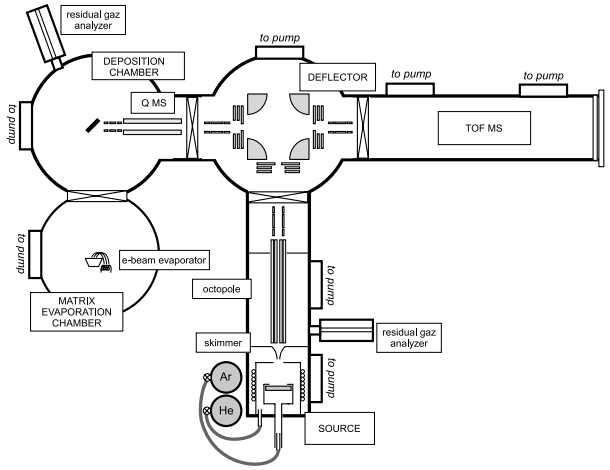

FIG. 1: Overview of the experimental setup.

II. EXPERIMENTAL REQUIREMENTS AND POSSIBILITIES

The aim of the experiment presented in this article is to extend the range of possible measurements to the range of clusters of a few to a few hundreds of atoms, where possible size-selected. Thus, for the first time, it is possible not only to characterize the cluster sizes to be deposited before and after deposition but to actually select them prior to deposition.
Experiments are to be performed on samples with either size-selected small clusters or well-defined distributions of larger clusters, where size selection is no longer feasible. The metal clusters are generated in the gas phase, mass-selected or at least narrowed down in their size distribution and embedded fragmentation-free in matrices stable at ambient conditions (i.e. metals or oxides) in order to be removed from the vacuum apparatus for further experiments. Additional demands include independent variation of cluster size and concentration and high cluster ion fluxes.
Scheduled experiments include optical absorption and fluorescence spectroscopy of small size-selected noble metal clusters embedded in quartz, magnetic measurements of transition metals (e.g. Co and Fe) in non-magnetic metallic matrices as well as experiments on transport properties such as giant magnetoresistance or extraordinary Hall effect. First results on magnetic measurements of distributions of Co clusters in copper demonstrating the feasibility of the projected research are presented in this article, further results on transport as well as optical properties will be published elsewhere [19].
In order to perform magnetic measurements with a commercial SQUID magnetometer, a saturation magnetization of the order of $M_{sat} = 10^{-5} emu$ is needed to unambiguously measure isothermal magetization or zero-field-cooled vs. field-cooled (ZFC-FC) curves. In a simplified estimation that Cobalt retains its full bulk magnetic moment of $\mu_{Co} = 1.715\mu_B$ even in small clusters this corresponds to $\sim 10^{15} atoms$, i.e. $\sim 3nA \cdot h$ for Co_{10}. Thus a cluster ion source yielding several Nanoampere per cluster size, stable over several hours is needed for this type of experiment.
An estimation for the optical density needed in order to be able to perform optical absorption spectroscopy yields up to one order of magnitude less cluster ion current needed, assuming a cross-section of $\sim 1 \mathring{A}^2/atom$.

III. EXPERIMENTAL SETUP

An overview of the experimental setup is shown in Fig. 1. The main parts are the cluster source, the transfer region including the quadrupole deflector, the time-of-flight mass spectrometer (TOF) and the deposition chamber.

A. Cluster source

Metal clusters are produced in a home-built magnetron cluster source following the setup developed by H. Haberland *et al.* [20]. A commercial 2"-magnetron (Kurt J. Lesker Ltd., Hastings, UK) has been adapted to allow floating of the anode with respect to ground potential and a directed gas flow between the two electrodes. A discharge of typically $5 - 60W$ is operated in an adjustable gas mixture of He and Ar at comparable fluxes around $300 sccm$ to eject metal atoms from the cathode into the gas phase. The gas flow over the sputtering target ensures at the same time cooling and clustering of the sputtered material as well as transport towards the exit of the aggregation tube. The clusters are swept through an adjustable diaphragm into the differentially pumped transfer stage. The magnetron is mounted in a liquid nitrogen cooled tube with variable distance between the discharge and the diaphragm. Variation of discharge power, gas flow conditions and the distance between magnetron and diaphragm allows the adjustment of the mean cluster size. Pressures in this region are typically 0.1-1 mbar. The surrounding vacuum chamber is pumped by a 1600 l/s turbomolecular pump resulting in pressures around $5 * 10^{-3} mbar$, depending on the source conditions chosen. The purity of the gases and especially of the supply lines has been found to be very important for reproducible cluster size generation.
The main advantages of the cluster source used are the known versatility concerning clustering metal used, the adjustable particle size (between one and tens of thousands of atoms) as well as high ion yields and currents. In our experiment the source is operated in the cation mode.

B. Transfer Region

Two independent setups are used to transfer the cluster ion beam through the subsequent differentially pumped chambers. One possibility used in order to easily characterize the cluster source is to skim off most of the rare gas $25mm$ downstream from the diaphragm, followed by regular ion optics like Einzel lenses and electrostatic deflectors. This setup is comparatively simple and robust but not optimal for high ion transfer efficiencies at masses below $\sim 4000amu$. Alternatively an octopole ion guide can be connected either directly after the aggregation tube exit or behind the skimmer, resulting in better transmission at the cost of possible discharges between octopole rods and source tube.
A quadrupole deflector mounted at the end of the transfer region allows to guide the cluster ions either towards the deposition chamber or to a time-of-flight mass spectrometer (TOF-MS). The neutral fraction of the cluster beam is discarded at this point.

C. Cluster ion beam characterization

The TOF mass spectrometer allows direct determination of the cluster size distribution and optimization of all necessary parameters. Only a small fraction of the ion beam is used, accordingly this technique is not suited for deposition. On the other hand it allows a much easier and faster optimization of the cluster source conditions than by quadrupole mass spectrometry. Typical mass spectra obtained are shown in Fig. 2.
Additionally to the qualitative characterization with the TOF, two Faraday detectors are mounted on the gate valves before and after the quadrupole deflector allowing the optimization of the ion current. The second detector is also equipped with a system of meshes in order to determine the kinetic energy distribution of the ion beam by retarding field analysis. The mean energy of the ions is defined by the potential of the source tube (typically $50eV$) plus a correction for larger clusters due to acceleration in the rare gas flow, standard deviations are normally $\sigma \approx 2eV$.

D. Cluster deposition

After optimization, the cluster ion beam is directed towards the deposition chamber. A quadrupole mass selector (QPS-9000, Extrel USA, up to $9000amu$) is mounted between the quadrupole deflector and the sample holder. It allows to either transmit an adjustable fraction of the whole cluster distribution (as a high-pass filter in rf-only mode or a band-pass filter with bad resolution) or the selection of a single cluster mass. The ion beam is then focussed onto a spot of $\sim 5mm$ diameter on the sample surface, whereby the potential of the sample may be used to decelerate the ions in order to ensure soft-landing

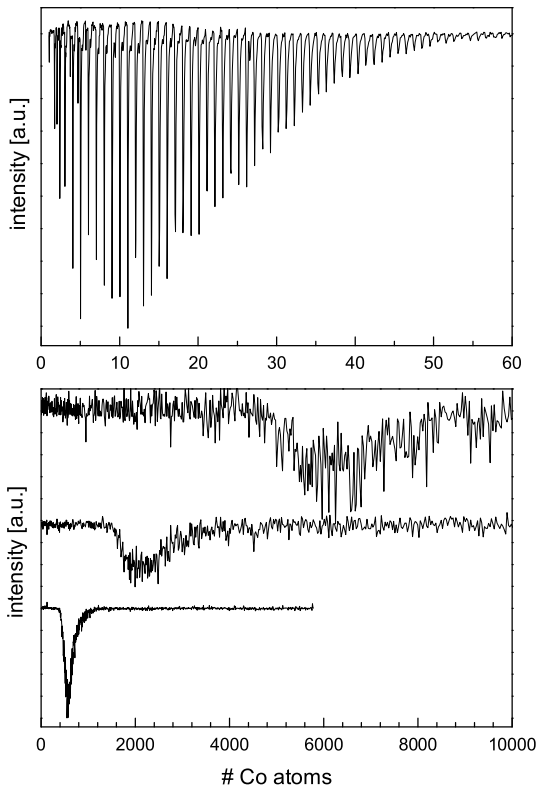

FIG. 2: Representative mass spectra of Cobalt clusters. The small satellite peaks in the upper spectrum are Co_nAr^+ complexes. The noise in the lower spectra is due to the reduced detection efficiency of the TOF-detector and does not reflect lower ion intensities.

conditions. If necessary, the cluster cations can also be neutralized at the surface using a tungsten filament.
The type of support used is chosen according to the desired experiments to be performed afterwards. For optical measurements quartz plates are used, for the determination of magnetic or transport properties we use stripes of conductive Polyimide (Kapton XC, Goodfellow, $40\mu m$ thickness, $370\Omega/cm^2$). The advantage of a slightly conductive support is that the surface potential is well defined and no additional neutralization is necessary, whereas at the same time the support does not interfere with transport measurements: the resistivity of the sample itself is more than two orders of magnitude smaller than that of the support. The magnetic response of the Kapton support has been measured and corrected for.
Up to four samples plus a Faraday detector of the same geometry can be mounted at 45° in a sample holder. At the same time as the cluster beam, the matrix is co-deposited from below. Matrix materials like metals (Cu, Ag, Al) or dielectrics as SiO_2 and Al_2O_3 are evaporated from a commercial 270°-electron gun evaporator (Fer-

rotec GmbH, Unterensingen, Germany). Typical cluster ion currents decelerated onto the surface are of the order of $10 - 20nA$ for the whole size distribution, independent of $\langle n \rangle$. Thus for small clusters ($n < 15$) currents of around $1nA$ per cluster size are achievable throughout several hours of deposition, allowing e.g. an optical density high enough for optical absorption measurements. Since the mean cluster size and the width of the distribution are directly linked, less current per size is available for larger clusters and we need to deposit several cluster sizes at the same time. The cluster ion current is monitored during deposition and the dilution of the sample is correspondingly adjusted via the flux of matrix particles as monitored by a quartz microbalance. So far all samples have been produced at room temperature, the possibility to heat or cool down the sample holder is provided.

Both sample holder and evaporator are mounted in UHV-chambers with a base pressure around $7*10^{-9}mbar$. During operation of the experiment the pressure in the deposition chamber rises to $\sim 5 * 10^{-8}mbar$ due to rare gas from the cluster source. Residual gas can be monitored with a $100amu$ quadrupole mass spectrometer connected to the deposition chamber. Without baking the pressure during operation is about a factor of 20 higher, mainly due to outgassing of heated components of the evaporator. This leads to a non-negligible rise in partial pressure of oxygen-containing molecules and thus to partial oxidization of the Cobalt clusters. Consequently a small bias shift in the magnetization curves [21] as well as a Cobalt-oxide peak in the XPS spectra were observed (see below) for the first samples produced and presented in this paper.

IV. RESULTS

Sample characterization possibilities as well as first results are presented in the following for the example of Cobalt clusters embedded in Copper matrices and their magnetic properties.

We prepared a series of samples with distributions of Cobalt clusters of different mean sizes embedded in Copper thin films. Both the atomic concentration as well as the film thickness were kept constant at $8at.\%$ Co and $50nm$, respectively. The mean cluster size deposited was $\langle n \rangle = 15, 600, 2300$ and $6500 atoms/cluster$, all distributions showing ratios between $\sigma/\langle n \rangle \approx 0.6 - 0.16$ for the smallest and largest cluster distributions used, respectively. The samples were capped by Cu films of $4nm$ thickness, enough to ensure oxidization protection after exposure to air [22].

It has to be borne in mind that, although thermodynamically immiscible at room temperature, a certain mobility at the interface has been observed previously ([23] and references therein). While local alloying due to atom exchange at the interface cannot be excluded, we rather expect capping of deposited clusters, as has been

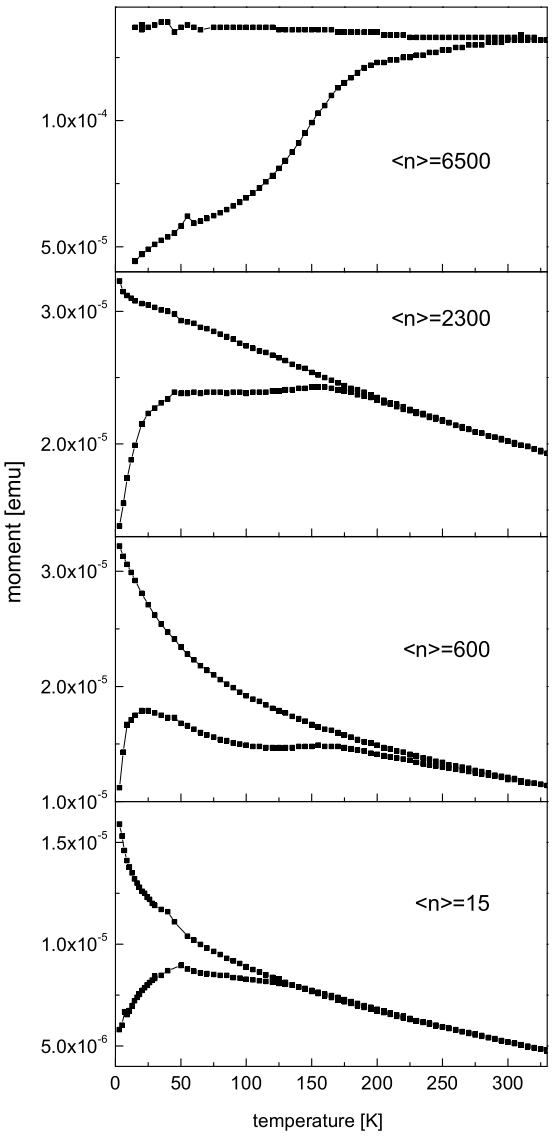

FIG. 3: Zero-field cooled and field cooled Magnetization curves for the different cluster sizes. Further details in the text.

observed for Co sub-monolayers on Cu [23]. This is also in accordance with theoretical calculations of the atomic deposition [24]. Both intermixing as well as capping up to the point of burrowing of the cluster into the surface [25] are enhanced at temperatures well above $300K$. Since our samples were prepared at room temperature, only small influences of intermixing are expected, in accordance with the results presented below.

X-ray photoelectron spectroscopy (XPS) at the Co-edge was performed on all samples, revealing significant oxidization ($\sim 50\%$), in accordance with bias shifts in field-cooled isothermal magnetization curves at low temperature (up to $450Oe$ for the largest clusters). This ox-

idization is most probably due to degassing of oxygen-containing molecules throughout operation.
High resolution transmission electron spectroscopy (HR-TEM) was performed on the sample of $\langle n \rangle = 6500$ in order to verify the structural integrity. In accordance with previous publications [26], an ordered crystalline lattice of both matrix and cluster was found showing well-separated, intact and near spherical clusters.
The larger clusters ($\langle n \rangle \geq 600$) can be considered well separated, as was verified by HR-TEM, nevertheless the dipolar interactions especially for the largest clusters can be estimated to possibly be as large as several meV, depending on both the exact distance as well as the amount of quenching of the magnetic moment per atom in the copper matrix [10]. This corresponds to a characteristic temperature of the order of $\sim 10K$, which is, however, not observed in our experimental data. More important is the interaction of the macrospin with the cluster crystalline lattice as demonstrated by the appearance of a blocking temperature T_B in zero-field magnetization curves.

The above-mentioned reasoning is underlined by magnetization measurements, performed with a 5T SQUID magnetometer (Quantum Design MPMS, San Diego, USA). Both isothermal M(H)-curves at different temperatures between $3K$ and $300K$ as well as zero-field cooled vs. field-cooled M(T) curves (ZFC-FC) were recorded (see Fig. 3). This standard procedure for superparamagnetic systems consists of cooling the sample in zero field, applying a small magnetic field in order to be able to measure the magnetization and then to raise the temperature while continuously measuring M(T). At low T the magnetic moment of an isolated cluster is frozen along its easy axis, the crystalline anisotropy prevents the macrospin from following the external field. As the temperature and thus the thermal energy is raised, more and more clusters in the ensemble may overcome this barrier and the mean magnetization rises. On the other hand at all T the thermal agitation competes with the alignment in the external field, thus reducing the overall magnetization. A maximum in this ZFC curve is attributed to the blocking temperature T_B of the cluster ensemble, the temperature at which thermal fluctuations and the interaction of the macrospin with the cluster crystalline lattice are of the same magnitude. ZFC-FC curves were measured between 200 and $500Oe$ for all samples to avoid field effects. The shoulder at $\sim 175K$ was observed in all samples and is attributed to the blocking temperature of the Cobalt-oxide layer [27, 28].
A clear difference between small and larger clusters deposited is observed:

- Samples with mean deposited cluster sizes of 6500; 2300 and 600 show, in accordance with the literature [29], a decreasing blocking temperature with size (see table I), accompanied by a decrease in coercive field at low temperatures;

- The sample with a mean deposited cluster size $\langle n \rangle = 15$ on the other hand yields both increased blocking temperature and coercive field.

We attribute these differences in magnetic response to the microscopic structure of our samples. At the same atomic concentration, larger clusters are isolated and interact, if at all, only weakly. Both blocking as well as hysteretic behavior are due to the interaction of the cluster macrospin with its crystalline lattice. The smaller clusters on the other hand interact more strongly since they are not as well separated. A statistical estimation yields a mean distance between two clusters of about three copper atomic diameters, thus many of the embedded clusters are thought to form three-dimensional structures with interacting magnetic moments. It is rather this inter-cluster coupling that leads to the non-reversible effects. This increase of T_B with increasing interaction as opposed to a spin-glass behavior has also been observed in recent Monte-Carlo-Simulations [30].

$\langle n \rangle$	6500	2300	600	15
T_B	$> 300K$	$65K$	$20K$	$50K$
$H_C(3K)$	$600Oe$	$550Oe$	$330Oe$	$530Oe$

TABLE I: Blocking temperatures and coercive fields for different cluster sizes as derived from ZFC M(T) and M(H) curves.

V. CONCLUSIONS

We have presented a new and unique experimental setup that allows us to prepare samples of well-characterized metal cluster size distributions in matrices stable at ambient conditions. This method can be applied to different cluster and matrix materials; cluster size selection is possible if less material is needed (e.g. optical spectroscopy). First results on Cobalt clusters of different size embedded in Copper matrices show the influence of particle size, oxidation and inter-cluster interactions on the magnetic properties. With this setup further experiments on optical and transport properties of different clusters in solid matrices are under way and will be published separately.

Acknowledgments

The authors would like to thank B. v. Issendorff for countless discussions and help concerning the cluster source, J.-P. Ansermet for the possibility to use his Magnetometer and M. Abid and S. Serrano-Guisan for their help with the XPS and TEM-data. The authors acknowledge the Swiss National Foundation for financial support.

[1] L. Peyser, A. Vinson, A. Bartko, and R. Dickson, Science **291**, 103 (2001).

[2] T.-H. Lee and R. Dickson, Proc. Natl. Acad. Sci. USA **100**, 3043 (2003).

[3] T. Gleitsmann, B. Stegemann, and T. Bernhardt, Appl. Phys. Lett. **84**, 4050 (2004).

[4] J. Bansmann, S. Baker, C. Binns, J. Blackman, J.-P. Bucher, J. Dorantes-Dávila, V. Dupuis, L. Favre, D. Kechkrakos, A. Kleibert, et al., Surf. Sci. Rep. **56**, 189 (2005).

[5] A. Perez, V. Dupuis, J. Tuaillon-Combes, L. Bardotti, B. Prével, E. Bernstein, P. Mélinon, L. Favre, A. Hannour, and M. Jamet, Adv. Eng. Mater. **7**, 475 (2005).

[6] C. Binns, S. Baker, S. Louch, F. Sirotti, H. Cruguel, P. Prieto, S. Thornton, and J. Bellier, Appl. Surf. Sci. **226**, 249 (2004).

[7] T. Nishizawa and K. Ishida, Bull. Alloy Phase Diagr. **5**, 161 (1984).

[8] P. Allia, M. Coisson, P. Tiberto, F. Vinai, M. Knobel, M. Novak, and W. Nunes, Phys. Rev. B **64**, 144420 (2001).

[9] A. Berkowitz, J. Mitchell, M. Carey, A. Young, S. Zhang, F. Spada, F. Parker, A. Hutten, and G. Thomas, Phys. Rev. Lett. **68**, 3745 (1992).

[10] D. Eastham, Y. Qiang, T. Maddock, J. Kraft, J.-P. Schille, G. Thompson, and H. Haberland, J. Phys. Condens. Matter **9**, L497 (1997).

[11] M. Jamet, W. Wernsdörfer, C. Thirion, D. Mailly, V. Dupuis, P. Mélinon, and A. Perez, Phys. Rev. Lett. **86**, 4676 (2001).

[12] S. Rubin, M. Holdenried, and H. Micklitz, Eur. Phys. J. B **5**, 23 (1998).

[13] The only exception to our knowledge is the experimental setup in the group of C. Binns where cluster size distributions in the range of $5nm$ are selected and deposited as ions [6].

[14] B. Wang, X. Chen, G. Chen, G. Wang, and J. Zhao, Surf. Rev. Lett. **11**, 15 (2004).

[15] Y. Xie and J. Blackman, Phys. Rev. B **66**, 155417 (2002).

[16] V. Stepanyuk, A. Baranov, D. Bazhanov, W. Hergert, and A. Katsnelson, Surf. Sci. **482-485**, 1045 (2001).

[17] J. Guevara, A. Llois, and M. Weissmann, Phys. Rev. Lett. **81**, 5306 (1998).

[18] X. Chuanyun, Y. Jinlong, D. Kaiming, and W. Kelin, Phys. Rev. B **55**, 3677 (1997).

[19] S. Serrano-Guisan, M. Abid, L. Gravier, J.-P. Ansermet, G. di Domenicantonio, M. Hillenkamp, and C. Félix, to be published.

[20] H. Haberland, M. Mall, M. Moseler, Y. Qiang, T. Reiners, and Y. Thurner, J. Vac. Sci. Technol. **12**, 2925 (1994).

[21] R. Morel, A. Brenac, and C. Pertemont, J. Appl. Phys. **95**, 3757 (2003).

[22] L. Gan, R. Gomez, C. Powell, R. McMichael, P. Chen, and J. W.F. Egelhoff, J. Appl. Phys. **93**, 8731 (2003).

[23] T. Bernhard, R. Pfandzelter, M. Gruyters, and H. Winter, Surf. Sci. **575**, 154 (2005).

[24] R. Pentcheva and M. Scheffler, Phys. Rev. B **65**, 155418 (2002).

[25] C. Zimmermann, M. Yeadon, K. Nordlund, J. Gibson, and R. Averback, Phys. Rev. Lett. **83**, 1163 (1999).

[26] J. Meldrim, Y. Qiang, Y. Liu, H. Haberland, and D. Sellmeyer, J. Appl. Phys. **87**, 7013 (2000).

[27] S. Gangopadhyay, G. Hadjipanayis, C. Sorensen, and K. Klabunde, J. Appl. Phys. **73**, 6964 (1993).

[28] M. Verelst, T. Ely, C. Amiens, E. Snoek, P. Lecante, A. Mosset, M. Respaud, J. Broto, and B. Chaudret, Chem. Mater. **11**, 2702 (1999).

[29] S. Blundell, *Magnetism in Condensed Matter* (Oxford University Press, 2001).

[30] J. García-Otero, M. Porto, J. Rivas, and A. Bunde, Phys. Rev. Lett. **84**, 167 (2000).